Cesium immobilization in metakaolin-based geopolymers elucidated by ^{133}Cs solid state NMR spectroscopy

M. Arbel-Haddad[1*], Y. Harnik[2], Y. Schlosser[3], A. Goldbourt[3*]

[1]Nuclear Research Center Negev, PO Box 9001, Beer Sheva 84901, Israel
[2]Israel Atomic Energy Commission (IAEC)
[3]School of Chemistry, Tel Aviv University, Ramat Aviv 6997801, Tel Aviv, Israel

[*] *MAH: arbel.haddad@gmail.com; AG: amirgo@tauex.tau.ac.il*

Abstract

Geopolymers are promising candidates for nuclear-waste immobilization, and more specifically for the immobilization of radioactive cesium. Low-Si metakaolin-based geopolymers cured at temperatures of 40°C in the presence of Cs ions generate a mixture of amorphous and crystalline phases including a Cs-bearing zeolite F phase. Using a combination of ^{133}Cs solid-state NMR and X-ray powder diffraction measurements we were able to show that Cs preferentially binds to zeolite F even when zeolite F is not the dominant phase in the matrix. Moreover, post-leaching NMR experiments indicate that zeolite F binds Cs more efficiently than the remaining crystalline or amorphous phases. Tailoring geopolymer formulations so that a large fraction of zeolite F is generated may therefore be a promising route for the production of immobilization matrices for cesium.

Introduction:

Geopolymers are a class of inorganic cementitious materials obtained by alkali activation of various aluminosilicate raw materials, either calcined clays such as metakaolin, or waste materials such as ashes (coal fly-ash, incinerator ashes) and slags. Whereas the preparation of geopolymers is similar to that of traditional Portland cement, their chemical nature is akin to that of zeolites, having an interconnected network of silicate and aluminate groups. The ion-binding preoperties of geoplymers, much like those of zeolites, are due to the negatively-charged tetrahedral aluminate groups. This property, together with their high chemical resistance, have made the geopolymers attractive candidates for waste immobilization applications, including nuclear waste[1–8].

Special attention has been given to the possibility of immobilizing wastes containing radioactive Cs species, which are often present in low-level nuclear waste. An example

from recent years is the need to immobilize municipal solid waste incineration ashes from the Fukoshima region, which have a high content of radioactive ^{134}Cs and ^{137}Cs following the nuclear accident in 2011[9–11]. Whereas most of the radioactive species found in low-level waste streams precipitate to form stable insolube compounds in the alkaline conditions afforded by cementitous materials, the immobilization of Cs is especially challenging due to the high solubility of most Cs compounds in both alkaline and acidic media. Mineral additives such as fly ash, slag and silica fume are often included in Portland cement based low-level radioactive waste formulations, and have been shown to improve wasteform performance, and more specifically Cs immobilization[12–14]. It was therefore suggested that geopolymers, which are produced by alkaline activation of these and similar pozzolonic materials, will be able to immobilize Cs ions efficiently[15,16].

The properties of geopolymer products vary depending on the composition of the aluminosilicate source material[17–20], the nature of the activating solution[21,22] and the curing conditions[23,24]. High-Si compositions (SiO_2:Al_2O_3 molar ratio > 2.0) form porous glass-like amorphous matrices[19,24], whereas low-Si compositions (SiO_2:Al_2O_3 molar ratio < 2.0) result in the formation of a composite structure, with crystalline domains, often zeolites, imbedded within the amorphous matrix[15,16,25–29] Most Cs-bearing geopolymers studied thus far had a relatively high SiO_2:Al_2O_3 ratio, yielding materials of a non-crystalline amorphous nature[3,5,30–34]. Heat treatment at elevated temperatures (~1000^{o}C) was suggested in order to form the Cs-bearing zeolite pollucite, $CsAlSi_2O_6$[31,33,35], or the feldspathoid phase $CsAlSiO_4$[33], which are known to be efficient immobilizing phases for Cs[36–38]. We have shown in a previous study that low-Si geopolymers prepared using mixed CsOH-NaOH solutions and cured at temperatures of 40^{o}C or lower may also yield a Cs-bearing crystalline phase, $(Cs,Na)AlSiO_4 \bullet nH_2O$, named zeolite-F[16]. Leaching experiments indicate a correlation between the formation of this Cs-bearing phase and the efficient and selective immobilization of Cs.

In most of the abovementioned studies, structural information concerning geopolymer structure was obtained from X-ray diffraction and scattering, FTIR spectroscopy, as well as porosity and surface area measurements. These experimental methods yield information concerning the ensemble of phases making up the geopolymer matrix. Direct probing of the chemical environment of Cs species within waste-incineration fly-ash based geopolymers was attempted by Shiota et al using Cs K-edge XAFS [9,10].

Recently, solid state ^{29}Si NMR has been used in order to probe the structural changes due to Cs incorporation in an alkali-activated blast furnace slag matrix, and its subsequent exposure to leaching conditions[39]. However, identification of the Cs binding sites, as well as their distribution between the different phases making up the geopolyer matrix is still lacking.

In the current study, ^{133}Cs magic angle spinning (MAS) solid-state NMR measurements were combined with structural information obtained from XRD data in order to characterize the binding sites of Cs within low-Si MK-based geopolymers. Furthermore, identification of the cesium binding sites allowed us to follow changes in the distribution of cesium between the different sites upon geopolymer leaching.

1. Materials and Methods:

1.1. Preparation of geopolymers:

Metakaolin (MK, PowerPozzTM) conforming to ASTM C-618, Class N Specifications for Natural and Calcined Pozzolans, was supplied by Advanced Cement Technologies (Blaine, Washington USA). The manufacturer's data for chemical composition and physical properties are presented in Tables 1 and 2.

Table 1: Chemical composition of raw metakaolin

Oxides, weight%										LOI[a]
SiO_2	Al_2O_3	Fe_2O_3	CaO	TiO_2	MgO	Na_2O	K_2O	P_2O_5	SO_3	<0.50%
51-53	42-44	<2.20	<0.2	<3.00	<0.10	<0.05	<0.40	<0.20	<0.50	

[a] LOI: loss on ignition, 950°C

Table 2: Physical characterization of raw metakaolin

BET [m^2/g]	Density [g/cm^3]	Particle size distribution		
		D10 [µm]	D50 [µm]	D90 [µm]
23.5	2.6	<2 µm	<4.5 µm	<25 µm

Activation solutions were prepared by mixing aqueous solutions of NaOH and CsOH. The molar fraction of CsOH in the mixed activating solutions, CsOH:MOH (M=Na+Cs), was varied between 2.5% to 100%, while the overall water to alkali molar ratio was kept at a constant value of H_2O:MOH=5.5, corresponding to hydroxide ion concentration of approximately 10M. The ratios between MK and the activating solutions were adjusted to obtain a M_2O:Al_2O_3 ratio of 1 (M= Na+Cs), assuming Al_2O_3 content of 44% in MK. The resulting cation content in each of the geopolymer preparations is given in Table 3.

MK was mixed manually with the activation solution at ambient temperature to yield a homogenous paste, which was cast into sealed polypropylene containers (50 ml) and cured at 40ºC±3 for 3 months, and consequently kept at room temperature.

Cured samples were ground manually by mortar and pestle to yield powder for XRD and NMR measurements as well as for leaching experiments.

Table 3: Cs and Na content of the different geopolymer preparations given as M_2O:Al_2O_3 molar ratios (M=Cs, Na) and weight fractions.

Sample name	M_2O:Al_2O_3 molar ratios		Cation content, weight %	
	Cs_2O:Al_2O_3	Na_2O:Al_2O_3	Cs	Na
2.5%Cs	0.025	0.975	1.4	9
5%Cs	0.050	0.950	2.8	8.5
7.5%Cs	0.075	0.925	3.8	8.3
10%Cs	0.100	0.900	5.4	7.9
25%Cs	0.250	0.750	11.8	6.3
50%Cs	0.500	0.500	21.5	3.9
75%Cs	0.750	0.250	29.9	1.8
100%Cs	1.000	---	36.9	---

1.2. XRD measurements:

XRD measurements were carried out using a PanAnalytical Empyrean Powder diffractometer with CuKα radiation at 40 kV, 30 mA, and a scanning rate of 0.49°/min from 2θ=5° to 2θ=60° (BGU, Beer Sheva, Israel).

1.3. NMR measurements:

^{133}Cs magic-angle spinning (MAS) single-pulse solid-state NMR spectra of ground samples were acquired on 9.4T and 14.1T AVIII Bruker spectrometers using triple-resonance 4 mm probes. ^{133}Cs shifts were referenced to a 1.0M solution of CsCl at 0 ppm. Additional explicit details are given in the figure captions.

1.4. Geopolymer leaching experiments:

Leaching experiments were performed for geopolymer samples containing 2.5%, 5%, 7.5%, 10%, 25%, 50%, 100% Cs. For each of the abovementioned compositions, two ground 1 g samples were contacted with 10 ml of deionized water for 24 hours. The mixture was shaken using a rotating shaker. The aqueous phase was separated from the solid sample after 24h. One sample of each composition had undergone a second leaching step, during which it was contacted with 10 ml of fresh deionized water for an additional period 22 hours (46 hours total).

The solid samples obtained after 24 or 46 hours of leaching were filtered using a Buchner funnel and washed with a small volume of deionized water, then dried under a hood for 48 hours. These samples were used for the post-leaching NMR measurements. For the 100%Cs geopolymer, a single post-leaching sample which had undergone the two-step 46 hours leaching procedure was obtained.

The fraction of Cs and Na leached from the samples after each leaching step was calculated by determining the concentration of Cs and Na in the aqueous leachant. Cs concentrations were determined by ICP-MS (NexION 300D, Perkin Elmer, USA) and Na concentrations were determined by ICP-OES (Optima 3300, Perkin Elmer, USA). Both were carried out at the Geological Survey of Israel, Jerusalem. Samples were diluted by a factor of 1000 or 5000 using 0.1 M HNO_3 for ICP-MS analysis, and spiked with 10 ppb Rh as an internal standard. The estimated error for Cs concentrations was less than 1%. For ICP-OES, samples were diluted by a factor of 10 using 0.1M HNO_3 and spiked with 5 ppm Sc as an internal standard. The estimated error for Na concentrations was 1%.

2. Results & discussion:

2.1. Xray diffraction measurements:

XRD diffraction patterns of geopolymer samples with varying Cs content are presented in Fig. 1. The diffraction pattern obtained for the 2.5%Cs sample (Cs/(Cs+Na)=2.5%) is essentially the same as that observed previously for similar samples containing 0% or 1% Cs[28]. The pattern shows distinct diffraction peaks due to zeolite A and zeolite X, which are superimposed upon a broad diffraction band centered at $2\theta=29.4$. This broad hump is due to an amorphous geopolymer phase. Diffraction peaks due to zeolite A and zeolite X were also observed in the XRD patterns of 5%Cs and 7.5%Cs samples.

However, for these two samples, peaks which correspond to a previously reported Cs-bearing zeolite (PDF#00-039-0131) were also observed. The Cs-bearing zeolite is the only crystalline phase indicated in the diffraction patterns of the 10%Cs sample and all samples with higher Cs content.

Barrer et al. were the first to report the formation of this Cs-bearing zeolite, having a chemical formula of $CsAlSiO_4 \bullet 1.2H_2O$, which was named zeolite Cs-D in their original publication[40]. It was initially prepared via hydrothermal synthesis from kaolinite and CsOH, but was later also obtained by ion exchange from its K-based analogue, $KAlSiO_4 \bullet 1.5H_2O$ (zeolite K-F)[40,41]. Powder diffraction data of the Cs form of this zeolite were later published by Kosorukov et al (PDF#00-039-0131[42]). The powder diffraction pattern of the Na analogue, PDF#00-039-0217, was calculated from single crystal diffraction data obtained by Baerlocher and Barrer[43]. Here we will refer to this zeolite structure as zeolite F, noting the Na and Cs analogues as zeoF(Na) and zeoF(Cs). Both the Na and Cs forms of zeolite F, as well as their Li[44], K[45] or Rb[43] analogs, are isostructural with the naturally occurring Ba-bearing zeolite edingtonite, with two alkali cations replacing the divalent Ba cation.

While the position of the diffraction peaks of zeoF(Na) and zeoF(Cs) are identical, changes in the relative intensities, which are due to the difference in electron density between Na and Cs as well as the different water content in the two homologous crystal structures, are evident[16]. Similar changes in the relative intensity of diffraction peaks can be seen by comparing the diffraction patterns of pollucite, the only naturally occurring Cs-bearing zeolite, and its Na-analog analcime[46].

The normalized diffraction patterns for samples containing 7.5%-100%Cs (Fig. 2) demonstrate the changes in the relative intensity of the diffraction peaks due zeolite F with increasing Cs content. The relative intensity of the diffraction peak at 2θ=12.42 (110) decreases with increasing Cs content, as do those for the peaks at 2θ=28.40, 31.07 ((222) and (312) reflections). In contrast, the relative intensities of diffraction peaks at 2θ=29.46, 25.03 ((114) and (220) reflections) increase with increasing Cs content. These changes in the diffraction patterns, moving away from the intensity ratios expected for zeoF(Na) towards those expected for zeoF(Cs), reflect a gradual increase in the Cs content within the zeolite F crystalline domains. The data also indicate an

increase in the contribution of the amorphous phase to the diffraction pattern with increasing Cs content.

The diffraction patterns with the highest Cs content (25%Cs and higher) display a diffraction peak at 2θ=19.82, which is not expected for the various zeoF phases. This peak may be due to a Cs or Na analog of the naturally occurring zeolite goosecreekite, $CaAl_2Si_6O_{16}•5H_2O$, which is the only aluminosilicate phase reported to have a diffraction peak at this angle.

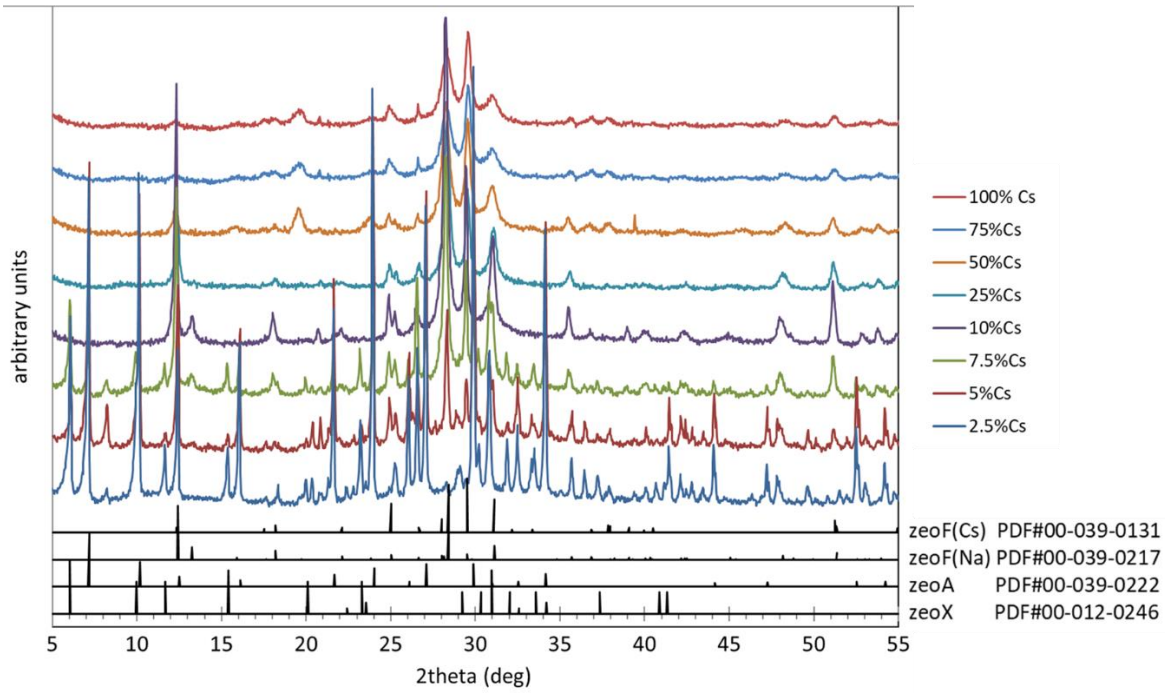

Figure 1: X-ray diffraction patterns of Cs-bearing MK-based geopolymers with varying Cs content. The diffraction lines are attributed to zeolite A, zeolite X, and zeolite F (Cs and Na forms)[47].

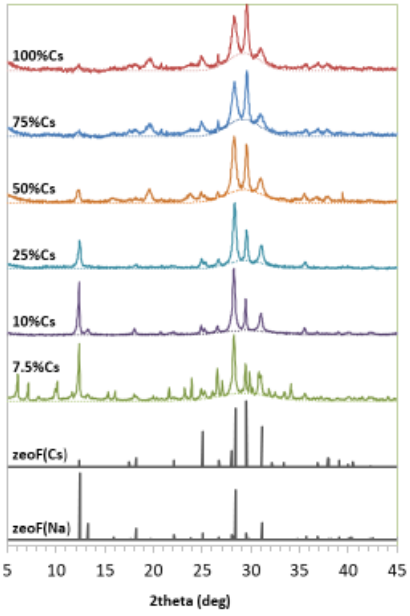

Figure 2: Changes in the relative intensity of diffraction peaks due to zeolite F with increasing Cs content in MK-based geopolymers. Background subtracted diffraction patterns were normalized according to maximum intensity. Dashed lines demonstrate the contribution of the amorphous phase to the diffraction patterns.

2.2. NMR measurements and comparison to XRD data:

The chemical shift of Cs obtained in ^{133}Cs MAS NMR measurements is known to be sensitive to the chemical environments within zeolite phases, and is influenced by its concentration within the specific phase, by the type of nearest neighbors, and by its hydration state[48–50]. In dehydrated zeolite samples Cs ions often have several resonance lines in the range of -60 to -150 ppm, depending on the size of the cages hosting the Cs ion (e.g. zeolite A and X[51], zeolite Y[49,52]). Upon rehydration, these lines shift to higher frequencies and merge into a single peak[49].

The ^{133}Cs MAS NMR spectra of the Cs-bearing MK-based geopolymers, which are presented in Fig. 3, report on the existence of several Cs sites within geopolymer matrices. The distribution of Cs between the different sites varies with Cs content. These changes can be correlated with the structural data obtained from XRD data, hence allowing for assignment of the features in the NMR spectra to the different phases making up the geopolymer matrix.

The two peaks observed in the ^{133}Cs NMR spectrum of the 2.5%Cs sample (bottom of Fig. 3) correspond from right to left to zeolites A (-3.5 ppm) and X (28.0 ppm). This identification is based on preliminary ^{133}Cs MAS NMR measurements of Cs-exchanged

zeolites A and X shown in Fig. 4. The chemical shifts obtained in the preliminary experiments are in a range that is characteristic of Cs ions residing in hydrated sites. Moreover, for both zeolite A and zeolite X, the Cs chemical shifts were found to increase with increasing Cs content, in agreement with previously reported data for zeolite X[48,50]. The chemical shifts of Cs in the 2.5%Cs geopolymer sample (Fig. 3) are similar to those obtained for the Cs-exchanged zeolites A and X with M=0.5 (Fig. 4). We can thus conclude that the Cs content in the crystalline phases is relatively high.

The ^{133}Cs NMR spectrum of the 5%Cs sample exhibits three peaks. We assign the new signal at 51.6 ppm to the zeolite F phase, which was observed in the powder diffraction pattern for of this sample. This assignment is supported by the increase in the relative intensity of this signal with increasing Cs content, which may be correlated with the increase in dominance of zeolite F diffraction peaks in the corresponding powder diffraction patterns (see Fig. 1). The remaining two peaks in the spectrum of the 5%Cs sample, -14.5 ppm and 19.4 ppm, correspond to Cs ions in the zeolite A and zeolite X phases, respectively. The shift of these peaks to lower values with respect to the 2.5%Cs sample indicate a lower Cs content within these phases, despite the higher overall content within the sample. It is also interesting to note that the area of the peak assigned to zeolite F (51.6 ppm) is of the same order of magnitude as that of the remaining two peaks, although the relative intensity of the diffraction peak due to the zeolite F in the XRD pattern of this sample is rather small. These results indicate preferential binding of Cs to zeolite F, and are in line with data published previously showing a decrease in Cs content in the pore solution and a decrease in Cs leaching in geopolymer samples following the formation of zeolite F within geopolymer samples[16].

The peak due to zeolite F is the dominant feature in the spectrum of the 7.5%Cs sample, with minor contributions from peaks due to zeolites A and X. This is in agreement with the increase in the intensity of XRD diffraction peaks of zeolite F for the sample of the same composition. The chemical shift of Cs in the zeolite F phase is similar to that observed for the 7.5%Cs sample, suggesting that the concentration of Cs cations in the zeolite F form is similar.

The spectra for samples with 10%-50%Cs all have a single peak assigned to zeolite F. The appearance of a single signal in the NMR spectra is in agreement with the XRD data, which indicate that zeolite F is the sole crystalline phase formed in this

compositional domain. A gradual increase in the corresponding ^{133}Cs shift from 51.6 ppm to 62 ppm can be observed, indicating a corresponding increase in Cs content within this phase. We also note a broadening of the line, probably caused by a larger distribution of the type of Cs sites occupied within zeolite F, due to a larger variation in Cs-nearest neighbor interactions. The increase in amorphous phase content, which is inferred from the XRD data, is not reflected in the NMR spectra for these compositions. This finding suggests that, here again, Cs preferentially resides within the zeolite F phase.

At 75%Cs we observe further broadening of the signal due to Cs in zeolite F (64.6 ppm) together with the appearance of several additional overlapping broad signals. A similar spectrum was observed for the 100%Cs sample, although in this case two distinct signals appear, which are due to the crystalline F phase (105.8 ppm) and a yet unidentified binding site (44.4 ppm). It is therefore evident that at these compositions Cs ions are no longer restricted to the zeolite F phase. XRD data for these compositions indicate a further increase in the amorphous fraction in the geopolymer matrices as well as the appearance of a new diffraction peak, which may be associated with the zeolite goosecreekite or a similar structure. The data from leaching experiments, which are presented in the following section, suggest that this site does not strongly bind Cs and is therefore more likely correlated with the amorphous phase that is dominant in the XRD pattern.

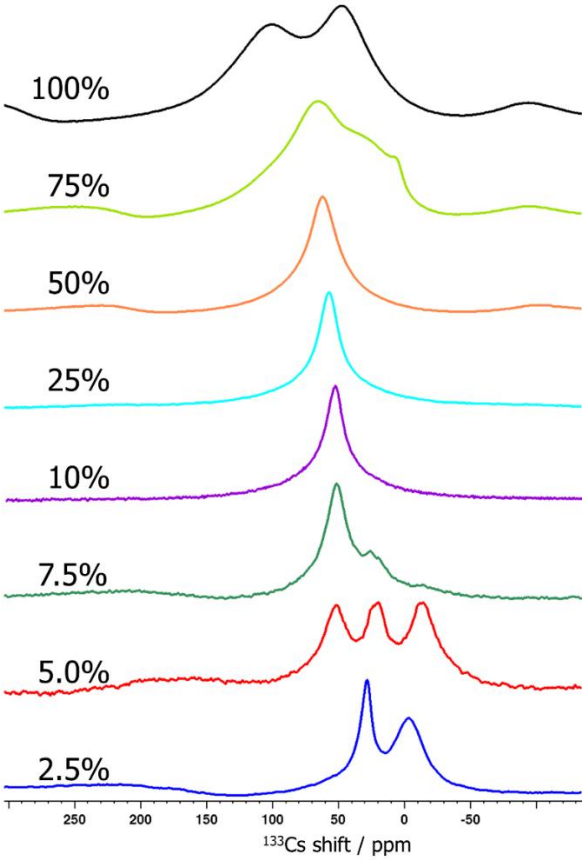

Figure 3: ^{133}Cs MAS NMR spectra of MK-based geopolymers with increasing Cs content. Spectra were acquired at a MAS rate of 13 kHz using a recycle delays of 1 sec (2.5-10%) and 0.25 sec (25-100%). No. of scans were 3072 (2.5%), 1536 (5-7.5%) and 512 (10-100%). All spectra were processed with line broadening of 100 Hz.

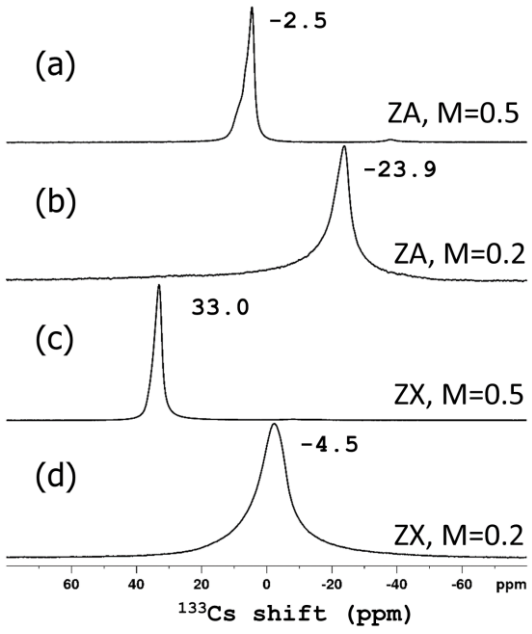

Figure 4: ^{133}Cs MAS NMR of Cs-exchanged zeolites A (a,b) and X (c,d). Zeolite A and zeolite X were obtained from Sigma-Aldrich in the Na form. Zeolite samples were contacted with a 0.1M CsCl solution for a period of 24 hours, washed in milipore water and then dried for 4 hrs at 95 ^{o}C. The extent of ion exchange in the zeolite sample was calculated from the decrease in Cs concentration in the equilibrated aqueous solution, as obtained by ion-chromatography according to a method described previously[16], and is given by M=[Cs]/[Cs]+[Na]. NMR spectra were obtained with repetition delays of 1s for (a, c, d) and 1.5s for (b). 128 scans were acquired for (a) and (c), 256 for (b) and 512 for (d). All spectra were processed with line broadening of 100 Hz.

2.3. Leaching experiments and post-leaching NMR measurements:

Identification of the different Cs sites as obtained by NMR allows us to track the leaching of Cs with site resolution. The cumulative fraction of Cs and Na ions leached into the aqueous phase after a single leaching step (24 hours) and two leaching steps (46 hours) from samples of selected compositions are presented in Table 4. The results show that the fraction of Cs leached was lower than 0.01 for the range of 5-25%Cs, increasing to ~0.05 for the 50%Cs sample, and slightly over 0.10 for the 100%Cs sample. Moreover, most of the Cs had leached out during the initial leaching step (24h). In contrast, the fraction of Na leached from the 2.5%Cs sample (97.5%Na) is close to 0.92 and decreases gradually down to 0.045 for the 50%Cs (50%Na) sample. At this composition the cumulative fractions of Cs and Na leached are similar.

Table 4: Cumulative fractions of Cs, Na and total alkalis (Cs+Na) leached during one step (24h) or two step (46 h) leaching experiments.

Sample name	Cumulative fraction leached					
	Cs		Na		Cs+Na	
	24h	48h	24h	48h	24h	48h
2.5%Cs	0.038	0.044	0.816	0.918	0.796	0.896
5.0%Cs	0.007	0.008	0.311	0.352	0.296	0.335
7.5%Cs	0.003	0.004	0.204	0.231	0.189	0.214
25%Cs	0.004	0.006	0.056	0.065	0.043	0.050
50%Cs	0.051	0.056	0.040	0.044	0.045	0.050
100%Cs	0.110	0.139	---	---	0.110	0.139

Fig. 5 shows a comparison of ^{133}Cs NMR spectra for selected samples following leaching times of 24 h and 46 h. Significant spectral changes were observed for samples with low Cs content, despite the low fraction of Cs leached (<0.05 for samples up to 25%Cs). As such small changes in the Cs concentration are not expected to affect the NMR spectrum significantly, we can conclude that the changes in the spectra at this

composition range are due to the significant leaching out of Na ions and their replacement by water molecules, which affect both the distribution and mobility of Cs ions within the geopolymer.

The post-leaching spectra of the 2.5%Cs sample (Fig. 5a) shows a two-fold increase in the relative intensity of the Cs peak due to zeolite A with respect to that of phase X (determined by peak integration), suggesting preferential migration of Cs ions into the zeolite A phase during the leaching process. Since a significant fraction of Na ions had leached out, the Cs ions were able to migrate to many newly available zeolite A sites. Thus, despite the higher content of Cs in Zeolite A, its local concentration decreases, as suggested from the lower chemical shift in the leached sample. It is not clear at this stage why the chemical shift of Cs in phase X is higher than in the non-leached sample; unlike zeolite A, this form is highly sensitive to many environmental conditions such as temperature and hydration[52]. The narrowing of the lines for both zeolite A and zeolite X can be attributed to the increased amount of water molecules or H_3O^+ ions replacing Na ions and thus increasing the mobility of Cs.

Similar effects can be seen for the 5%Cs sample (Fig. 5b); normalization of the spectra to the intensity of the zeolite A peak allows us to demonstrate a decrease in the relative intensity of the zeolite X site upon leaching. Moreover, the relative intensity of the signal due to zeolite F increased (the signal after 24 h seems at lower intensity, but is broader than the signal of the non-leached sample), suggesting preferential binding of Cs ions to zeolite F. Since the fraction of Na leached is significantly smaller than in the case of the 2.5%Cs sample, no apparent change of Cs concentration is observed for F and A phases. Another observation is the appearance of a new site with a chemical shift of 33.9 ppm. This site could be attributed to Cs located at one of two different chemical environments, which are available in zeolite X. It is possible that preferential depletion of Na from one of the two cavities results in changes to the local environment of the remaining Cs ions. However, we do not have further evidence for this hypothesis.

The zeolite F site remains the dominant feature in the spectrum of the 7.5%Cs samples following leaching (Fig. 5c), with small contributions from zeolites X and A. The extent of leaching from this sample was much smaller than from the previous two samples (cumulative fractions leached were 0.20 for Na ions and 0.003 for Cs ions). Thus, no significant spectral changes are observed for the different leaching times. Similarly,

leaching from the 25% and 50% samples (Fig. 5d and e) is very minor (~cumulative fractions of 0.05 for both ions from the 50%Cs sample, 0.005 for Cs ion from the 25%Cs sample), thus no changes are observed in the spectrum.

A significant change in the NMR spectrum occurred upon leaching the 100%Cs sample (Fig. 5f). In this case, a substantial amount of Cs had leached from the sample, and clearly it has preferentially leached out of the site with the lower chemical shift. We suggest that this signal corresponds to Cs residing in the amorphous fraction of the sample, which binds Cs less efficiently than the crystalline zeolite F phase.

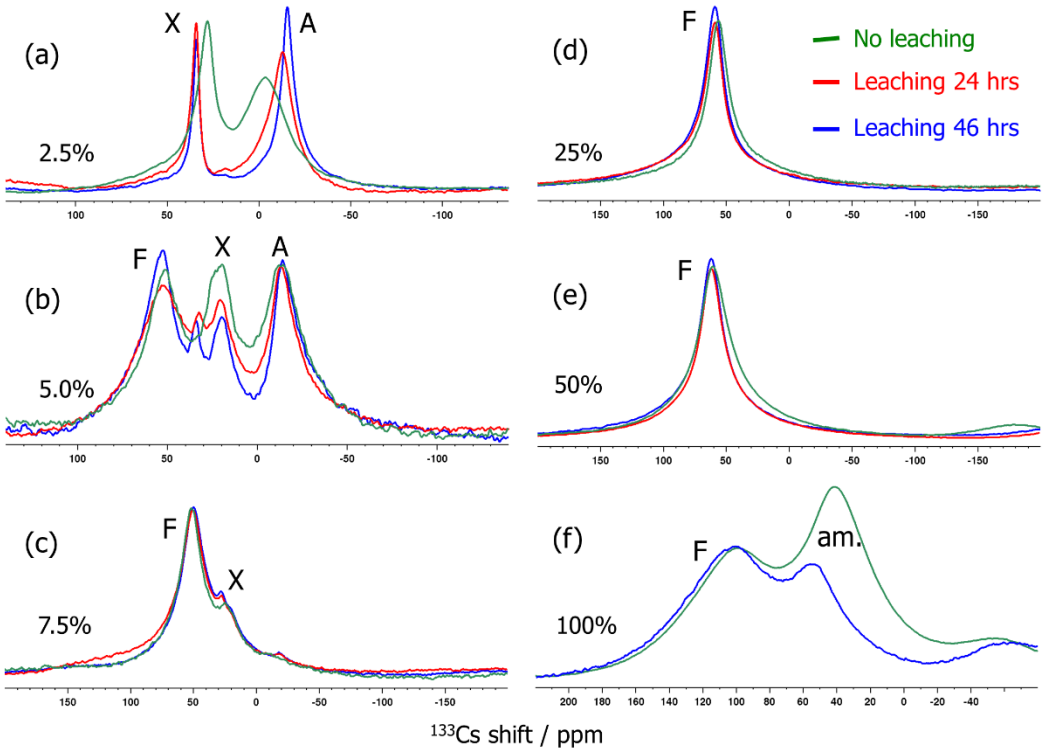

Figure 5: ^{133}Cs single-pulse MAS NMR spectra acquired following the two leaching steps (24h, 46h) compared to spectra of the same samples before leaching (same spectra as in Fig. 4). For the leached samples, spectra were acquired at a MAS rate of 14 kHz (2.5-7.5%) and 13 kHz (25-100%) using recycle delays of 1 sec. Number of scans were 3072 (2.5%), 1536 (5-7.5%), 512 (25%), 600(50%-24h), 128(50%-46h), and 64(100%-46h). All spectra were processed with line broadening of 100 Hz.

3. Summary and Conclusion

Correlation of ^{133}Cs NMR measurements with structural data obtained from XRD allowed us, for the first time, to assign the different signals in the NMR spectra to specific binding sites within a composite crystalline-amorphous geopolymer matrix. Moreover, using ^{133}Cs NMR data we were able to identify changes in the distribution of Cs ions between different phases following leaching experiments.

NMR data indicated that a significant part of the Cs ions is incorporated into the zeolite F phase in the 5%Cs sample, which contains only 2.8wt% Cs, although this is not the most dominant phase within the geopolymer matrix. A clear preference for incorporation of Cs into the zeolite F phase over the amorphous matrix is observed for the 10%Cs-50%Cs samples. Significant presence of Cs ions in the amorphous phases was observed only in 75%Cs and 100%Cs samples, probably due to exhaustion of the available zeolite F binding sites.

The ability to identify the Cs binding sites was found to be useful in order to identify changes in Cs ion distribution within the geopolymer following leaching experiments. At low Cs content, a significant leaching of Na ions most probably results in their replacement by water molecules, allowing increased mobility and redistribution of the Cs ions. When zeolite F sites are available, Cs ions migrate to this phase. In the 100%Cs sample, where a more significant amount of Cs leaches out, NMR data indicate again that Cs is retained by the zeolite F phase and leaches preferentially out of the amorphous phase.

Our results show that better insight into Cs immobilization is obtained by combining X-ray powder diffraction and solid-state NMR measurements. While XRD reveals the different phases in the geopolymer matrix, the information it provides concerning Cs ion distribution between these phases is limited. Such information is easily obtained by ^{133}Cs NMR. In the case studied here, the data afforded by ^{133}Cs solid-state NMR demonstrated the preferential incorporation of Cs in zeolite F, as well as its retention within this phase during the applied leaching test, thus confirming that the formation of this crystalline phase within a composite geopolymer matrix increases its efficiency for cesium immobilization. Tailoring geopolymer formulations so that a large fraction of Cs-binding phases are generated may therefore be a promising route for the production of immobilization matrices for cesium.

4. References

(1) Khalil, M. Y.; Merz, E. Immobilization of Intermediate-Level Wastes in Geopolymers. *J. Nucl. Mater.* **1994**, *211* (2), 141–148. https://doi.org/10.1016/0022-3115(94)90364-6.

(2) Aly, Z.; Vance, E. R.; Perera, D. S.; Hanna, J. V.; Griffith, C. S.; Davis, J.; Durce, D. Aqueous Leachability of Metakaolin-Based Geopolymers with Molar Ratios of Si/Al = 1.5-4. *J. Nucl. Mater.* **2008**, *378* (2), 172–179. https://doi.org/10.1016/j.jnucmat.2008.06.015.

(3) Blackford, M. G.; Hanna, J. V.; Pike, K. J.; Vance, E. R.; Perera, D. S. Transmission Electron Microscopy and Nuclear Magnetic Resonance Studies of Geopolymers for Radioactive Waste Immobilization. *J. Am. Ceram. Soc.* **2007**, *90* (4), 1193–1199. https://doi.org/10.1111/j.1551-2916.2007.01532.x.

(4) Chervonnyi, A. D.; Chervonnaya, N. A. Geopolymeric Agent for Immobilization of Radioactive Ashes after Biomass Burning. *Radiochemistry* **2003**, *45* (2), 182–188. https://doi.org/10.1023/A:1023845628670.

(5) Li, Q.; Sun, Z.; Tao, D.; Xu, Y.; Li, P.; Cui, H.; Zhai, J. Immobilization of Simulated Radionuclide 133Cs+ by Fly Ash-Based Geopolymer. *J. Hazard. Mater.* **2013**, *262*, 325–331. https://doi.org/10.1016/j.jhazmat.2013.08.049.

(6) Fernandez-Jimenez, A.; MacPhee, D. E.; Lachowski, E. E.; Palomo, A. Immobilization of Cesium in Alkaline Activated Fly Ash Matrix. *J. Nucl. Mater.* **2005**, *346* (2–3), 185–193. https://doi.org/10.1016/j.jnucmat.2005.06.006.

(7) Chen, S.; Wu, M.; Zhang, S. Mineral Phases and Properties of Alkali-Activated Metakaolin-Slag Hydroceramics for a Disposal of Simulated Highly-Alkaline Wastes. *J. Nucl. Mater.* **2010**, *402* (2–3), 173–178. https://doi.org/10.1016/j.jnucmat.2010.05.015.

(8) Jang, J.; Park, S.; Lee, H. Cesium and Strontium Retentions Governed by Aluminosilicate Gel in Alkali-Activated Cements. *Materials (Basel).* **2017**, *10* (4), 447. https://doi.org/10.3390/ma10040447.

(9) Shiota, K.; Nakamura, T.; Takaoka, M.; Nitta, K.; Oshita, K. Kinetics of Cs

Species in an Alkali-Activated Municipal Solid Waste Incineration Fly Ash and Pyrophyllite-Based System Using Cs K-Edge in Situ X-Ray Absorption Fi Ne Structure Analysis. *Spectrochim. Acta Part B At. Spectrosc.* **2017**, *131*, 32–39. https://doi.org/10.1016/j.sab.2017.03.003.

(10) Shiota, K.; Nakamura, T.; Oshita, K.; Fujimori, T. Quantitative Cesium Speciation and Leaching Properties in Alkali-Activated Municipal Solid Waste Incineration Fly Ash and Pyrophyllite-Based Systems. *Chemosphere* **2018**, *213*, 578–586. https://doi.org/10.1016/j.chemosphere.2018.09.097.

(11) Jing, Z.; Yuan, Y.; Hao, W.; Miao, J. Synthesis of Pollucite with Cs-Polluted Incineration Ash Mixed with Soil for Immobilization of Radioactive Cs. *J. Nucl. Mater.* **2018**, *510*, 141–148. https://doi.org/10.1016/j.jnucmat.2018.07.047.

(12) Ojovan, M. I.; Lee, W. E. *An Introduction to Nuclear Waste Immobilisation*, Second Edi.; Elsevier, Amsterdam, 376 p., 2014.

(13) Drace, Z.; Ojovan, M. I. The Behaviours of Cementitious Materials in Long Term Storage and Disposal: An Overview of Results of the IAEA Coordinated Research Project. In *Materials Research Society Symposium Proceedings*; IAEA, Vienna, 2009; Vol. 1193, pp 663–672. https://doi.org/10.1557/proc-1193-663.

(14) Bar-Nes, G.; Katz, A.; Peled, Y.; Zeiri, Y. The Mechanism of Cesium Immobilization in Densified Silica-Fume Blended Cement Pastes. *Cem. Concr. Res.* **2008**, *38* (5), 667–674. https://doi.org/10.1016/j.cemconres.2007.09.017.

(15) Ofer-Rozovsky, E.; Arbel Haddad, M.; Bar Nes, G.; Katz, A. The Formation of Crystalline Phases in Metakaolin-Based Geopolymers in the Presence of Sodium Nitrate. *J. Mater. Sci.* **2016**, *51* (10), 4795–4814. https://doi.org/10.1007/s10853-016-9767-0.

(16) Arbel Haddad, M.; Ofer-Rozovsky, E.; Bar-Nes, G.; Borojovich, E. J. C.; Nikolski, A.; Mogiliansky, D.; Katz, A. Formation of Zeolites in Metakaolin-Based Geopolymers and Their Potential Application for Cs Immobilization. *J. Nucl. Mater.* **2017**, *493*, 168–179. https://doi.org/10.1016/j.jnucmat.2017.05.046.

(17) Xu, H.; van Deventer, J. S. . The Geopolymerisation of Aluminosilicate Minerals. *Int. J. Miner. Process.* **2000**, *59* (3), 247–266.

(18) Komnitsas, K.; Zaharaki, D. Geopolymerisation: A Review and Prospects for the Minerals Industry. *Miner. Eng.* **2007**, *20* (14), 1261–1277. https://doi.org/http://dx.doi.org/10.1016/j.mineng.2007.07.011.

(19) Duxson, P.; Fernandez-Jimenez, A.; Provis, J. L.; Lukey, G. C.; Palomo, A.; Deventer, J. S. J. Geopolymer Technology: The Current State of the Art. *J. Mater. Sci.* **2007**, *42* (9), 2917–2933. https://doi.org/10.1007/s10853-006-0637-z.

(20) Diaz, E. I.; Allouche, E. N.; Eklund, S. Factors Affecting the Suitability of Fly Ash as Source Material for Geopolymers. *Fuel* **2010**, *89* (5), 992–996. https://doi.org/10.1016/j.fuel.2009.09.012.

(21) Fernández-Jiménez, A.; Palomo, A. Composition and Microstructure of Alkali Activated Fly Ash Binder: Effect of the Activator. *Cem. Concr. Res.* **2005**, *35* (10), 1984–1992. https://doi.org/10.1016/j.cemconres.2005.03.003.

(22) Aiello, R.; Crea, F.; Nastro, A.; Subotic, B.; Testa, F. Influence of Cations on the Physicochemical and Structural Properties of Aluminosilicate Gel Precursors . Chemical and Thermal Properties. *Zeolites* **1991**, *11*, 767–775.

(23) Rovnaník, P. Effect of Curing Temperature on the Development of Hard Structure of Metakaolin-Based Geopolymer. *Constr. Build. Mater.* **2010**, *24* (7), 1176–1183. https://doi.org/10.1016/j.conbuildmat.2009.12.023.

(24) Soutsos, M.; Boyle, A. P.; Vinai, R.; Hadjierakleous, A.; Barnett, S. J. Factors Influencing the Compressive Strength of Fly Ash Based Geopolymers. *Constr. Build. Mater.* **2016**, *110*, 355–368. https://doi.org/10.1016/j.conbuildmat.2015.11.045.

(25) Provis, J. L.; Lukey, G. C.; Van Deventer, J. S. J. Do Geopolymers Actually Contain Nanocrystalline Zeolites? A Reexamination of Existing Results. *Chem. Mater.* **2005**, *17* (12), 3075–3085. https://doi.org/10.1021/cm050230i.

(26) Silva, P.; Sagoecrenstil, K.; Sirivivatnanon, V. Kinetics of Geopolymerization: Role of Al2O3 and SiO2. *Cem. Concr. Res.* **2007**, *37* (4), 512–518.

https://doi.org/10.1016/j.cemconres.2007.01.003.

(27) Fernández-Jiménez, A.; Monzo, M.; Vicent, M.; Barba, A.; Palomo, A. Alkaline Activation of Metakaolin-Fly Ash Mixtures: Obtain of Zeoceramics and Zeocements. *Microporous Mesoporous Mater.* **2008**, *108* (1–3), 41–49. https://doi.org/10.1016/j.micromeso.2007.03.024.

(28) Ofer-Rozovsky, E.; Arbel Haddad, M.; Bar-Nes, G.; Borojovich, E. J. C.; Binyamini, A.; Nikolski, A.; Katz, A. Cesium Immobilization in Nitrate-Bearing Metakaolin-Based Geopolymers. *J. Nucl. Mater.* **2019**, *514*, 247–254. https://doi.org/10.1016/j.jnucmat.2018.11.003.

(29) Rożek, P.; Król, M.; Mozgawa, W. Geopolymer-Zeolite Composites: A Review. *J. Clean. Prod.* **2019**, *230*, 557–579. https://doi.org/10.1016/j.jclepro.2019.05.152.

(30) Bell, J. L.; Driemeyer, P. E.; Kriven, W. M. Formation of Ceramics from Metakaolin-Based Geopolymers: Part I-Cs-Based Geopolymer. *J. Am. Ceram. Soc.* **2009**, *92* (1), 1–8. https://doi.org/10.1111/j.1551-2916.2008.02790.x.

(31) Bell, J. L.; Sarin, P.; Provis, J. L.; Haggerty, R. P.; Driemeyer, P. E.; Chupas, P. J.; Van Deventer, J. S. J.; Kriven, W. M. Atomic Structure of a Cesium Aluminosilicate Geopolymer: A Pair Distribution Function Study. *Chem. Mater.* **2008**, *20* (14), 4768–4776. https://doi.org/10.1021/cm703369s.

(32) Berger, S.; Frizon, F.; Joussot-Dubien, C. Formulation of Caesium Based and Caesium Containing Geopolymers. *Adv. Appl. Ceram.* **2009**, *108* (7), 412–417. https://doi.org/10.1179/174367609X422072.

(33) Chlique, C.; Lambertin, D.; Antonucci, P.; Frizon, F.; Deniard, P. XRD Analysis of the Role of Cesium in Sodium-Based Geopolymer. *J. Am. Ceram. Soc.* **2015**, *98* (4), 1308–1313. https://doi.org/10.1111/jace.13399.

(34) Bernal, S. A.; Van Deventer, J. S. J.; Provis, J. L. What Happens to 5 Year Old Metakaolin Geopolymers' the Effect of Alkali Cation. In *Calcined Clays for Sustainable Concrete*; Scrivner, K., Favier, A., Eds.; 2015; pp 315–321.

(35) Bell, J. L.; Driemeyer, P. E.; Kriven, W. M. Formation of Ceramics from Metakaolin-Based Geopolymers. Part II: K-Based Geopolymer. *J. Am. Ceram.*

Soc. **2009**, *92* (3), 607–615. https://doi.org/10.1111/j.1551-2916.2008.02922.x.

(36) Gallagher, S. A.; Mccarthy, G. J. Preparation and X-Ray Characterization of Pollucite (CsA1Si206). *Mater. Res.* **1981**, *43*, 1773–1777.

(37) Xu, H. W.; Navrotsky, A.; Balmer, M. L.; Su, Y. L. Crystal Chemistry and Phase Transitions in Substituted Pollucites along the CsAlSi2O6-CsTiSi2O6.5 Join: A Powder Synchrotron X-Ray Diffractometry Study. *J. Am. Ceram. Soc.* **2002**, *85*, 1235–1242.

(38) Komarnenl, S.; Mccarthy, G. J.; Gallagher, S. A. Cation Exchange Behaviour of Synthetic Cesium Aluminosilicates. *Inorg. Nucl. Chem. Lett.* **1978**, *14*, 173–177.

(39) Komljenović, M.; Tanasijević, G.; Džunuzović, N.; Provis, J. L. Immobilization of Cesium with Alkali-Activated Blast Furnace Slag. *J. Hazard. Mater.* **2020**, *388*, 121765. https://doi.org/10.1016/j.jhazmat.2019.121765.

(40) Barrer, R. M.; Cole, J. F.; Sticher, H. Chemistry of Soil Minerals. Part V. Low Temperature Hydrothermal Transformations of Kaolinite. *J. Chem. Soc. A Inorganic, Phys. Theor.* **1968**, 2475. https://doi.org/10.1039/j19680002475.

(41) Barrer, R. M.; Munday, B. M. Cation Exchange in the Synthetic Zeolite K-F. *J. Chem. Soc. A Inorganic, Phys. Theor.* **1971**, 2914. https://doi.org/10.1039/j19710002914.

(42) Kosorukov, A. A.; Nadel, L. G. On Zeolite K-F and Its Rubidium and Cesium Analogs. *Zh. Neorg. Khim.* **1985**, *30* (7), 1690–1693.

(43) Baerlocher, C.; Barrer, R. M. The Crystal Structure of Synthetic Zeolite F. *Zeitschrift fur Krist. - New Cryst. Struct.* **1974**. https://doi.org/10.1524/zkri.1974.140.1-2.10.

(44) Matsumoto, T.; Miyazaki, T.; Goto, Y. Synthesis and Characterization of Li-Type EDI Zeolite. *J. Eur. Ceram. Soc.* **2006**, *26* (4–5), 455–458. https://doi.org/10.1016/j.jeurceramsoc.2005.06.003.

(45) Tambuyzer, E.; Bosmans, H. J. The Crystal Structure of Synthetic Zeolite K–F. *Acta Crystallogr. Sect. B Struct. Crystallogr. Cryst. Chem.* **1976**, *32* (6),

1714–1719. https://doi.org/10.1107/S0567740876006286.

(46) Presser, V.; Kloužková, A.; Mrázová, M.; Kohoutková, M.; Berthold, C. Micro-Raman Spectroscopy on Analcime and Pollucite in Comparison to X-Ray Diffraction. *J. Raman Spectrosc.* **2008**. https://doi.org/10.1002/jrs.1886.

(47) International center for diffraction data https://www.icdd.com/.

(48) Chang Kim, J.; Li, H.-X.; Chen, C.-Y.; Davis, M. E. Base Catalysis by Intrazeolitic Cesium Oxides. *Microporous Mater.* **1994**, *2* (5), 413–423. https://doi.org/10.1016/0927-6513(94)00008-5.

(49) Koller, H.; Burger, B.; Schneider, A. M.; Engelhardt, G.; Weitkamp, J. Location of Na+ and Cs+ Cations in CsNaY Zeolites Studied by 23Na and 133Cs Magic-Angle Spinning Nuclear Magnetic Resonance Spectroscopy Combined with X-Ray Structure Analysis by Rietveld Refinement. *Microporous Mater.* **1995**, *5* (4), 219–232. https://doi.org/10.1016/0927-6513(95)00061-5.

(50) Yagi, F.; Kanuka, N.; Tsuji, H.; Nakata, S.; Kita, H.; Hattori, H. 133Cs and 23Na MAS NMR Studies of Zeolite X Containing Cesium. *Microporous Mater.* **1997**, *9* (5–6), 229–235. https://doi.org/10.1016/S0927-6513(96)00113-7.

(51) Ibarra, I. A.; Lima, E.; Loera, S.; Bosch, P.; Bulbulian, S.; Lara, V. II. Cesium Leaching in CsA and CsX Zeolites: Use of Blocking Agents to Inhibit the Cesium Cation Mobility. *J. Phys. Chem. B* **2006**, *110* (42), 21086–21091. https://doi.org/10.1021/jp061926h.

(52) Norby, P.; Poshni, F. I.; Gualtieri, A. F.; Hanson, J. C.; Grey, C. P. Cation Migration in Zeolites: An in Situ Powder Diffraction and MAS NMR Study of the Structure of Zeolite Cs(Na)−Y during Dehydration. *J. Phys. Chem. B* **1998**, *102* (5), 839–856. https://doi.org/10.1021/jp9730398.